

# PHASE DIAGRAMS IN HIGHER DIMENSIONAL U(1) LATTICE GAUGE THEORY\*

BRYAN BARMORE<sup>†</sup>

Department of Physics, College of William and Mary  
Williamsburg, Virginia 23187, USA  
email: barmore@mail.phy.ornl.gov

*(Received February 25, 1999)*

In five or more dimensions, U(1) lattice gauge theory shows a strong first-order phase transition and metastable states in the region of the transition. Monte Carlo calculations carried out in dimensions up to seven illustrate this behavior. These metastable states are well reproduced by gauge-fixed mean-field theory for the “superheated state” ( $\beta < \beta_c$ ) and by Padé approximants to the strong-coupling expansion for the “supercooled state” ( $\beta > \beta_c$ ). In analogy to a Van der Waal’s system, a cubic equation of state is employed to connect the two metastable states in both the Monte Carlo and analytic calculations. A Maxwell construct is developed allowing for the identification of the transition point and a complete, analytic description of the phase diagram in five and higher dimensions.

PACS numbers: 11.15.Ha, 11.15.Tk, 11.15.Me, 02.70.Lq

## 1. Introduction

It is widely accepted that the fundamental description of nuclear physics comes from quantum chromodynamics (QCD). However, QCD is non-perturbative at the energy scales of interest to nuclear physicists. Alternate methods must be developed to describe QCD at these low energies. The most promising development for an exact solution has been lattice gauge theory [1] where QCD is modeled on a discrete space-time lattice. The resulting denumerable degrees of freedom and ultraviolet cut-off allow for both formal study and numeric investigation. The continuum limit is approached with the help of the renormalization group, and physical observables are predicted. As computing power increases and algorithms become more efficient,

---

\* This paper has been recommended for publication by J.D. Walecka, a member of the International Editorial Council of Acta Physica Polonica B.

<sup>†</sup> Present address: Joint Institute for Heavy-Ion Research, Oak Ridge Tennessee 37831.

more and more accurate results can be obtained numerically. However, it is always profitable to have analytic techniques that can offer physical insight and check numeric results. The goal of this paper is to describe a method of combining two analytic methods into a complete description of the phase diagram for arbitrary dimensions in a  $U(1)$  pure gauge theory. In addition, Monte Carlo calculations are extended to seven dimensions to compare with the analytic results.

The  $U(1)$  lattice gauge theory has been well studied, both analytically [2–8] and numerically [9–13]. While not having the physical relevance of a non-Abelian theory like  $SU(3)$ , the  $U(1)$  theory provides a good testing ground for lattice methods and the study of lattice artifacts. Understanding what the lattice regularization does in a simple model group like  $U(1)$  can help to better the understanding of these effects on the more physically interesting groups.

In the continuum limit, a pure  $U(1)$  gauge theory becomes QED without fermions, *i.e.*, a gas of non-interacting photons. However, the lattice regularization introduces a coupling between the photon fields to infinite order in the coupling constant. Therefore, this becomes a rich, complex theory. In four dimensions a  $U(1)$  lattice gauge theory exhibits a phase transition as a function of coupling. In the groups  $SU(2)$  and  $SU(3)$ , one needs to go to at least five dimensions before seeing a phase transition. In addition, the study of monopole condensation in  $U(1)$  LGT can offer insight into color confinement in QCD [12].

Many analytic techniques have been developed to tackle  $U(1)$  LGT. They include both the strong-coupling [3, 4, 14, 15] and weak-coupling [5] expansions, mean-field theory (MFT) [1, 2, 7, 14–16] and interpolating Lagrangians [8, 17]. The method described below constructs a bridge between two of these, the strong-coupling expansion and mean-field theory, resulting in a description of the phase diagram for all values of the coupling.

Several refinements are implemented beyond the basic ideas of the SCE and MFT. Padé approximants can be used to improve the behavior of the SCE near the transition region (see Refs. [4, 10]). While many suggestions have been made to improve MFT, only the simplest will be used here. These include working in higher numbers of dimensions and gauge fixing. These improvements are more than sufficient for use with this new bridging technique.

For  $d \geq 5$ , the  $U(1)$  gauge theory exhibits a strong first-order phase transition with long-lived, metastable states. The phase diagram is reminiscent of the  $P$ – $V$  diagram for a Van der Waal’s gas. Therefore, we fit the metastable phases with a cubic equation of state. This introduces an additional unphysical region with negative specific heat analogous to the state of negative compressibility in the Van der Waal’s gas. The relative free en-

ergy of the phases is calculated and minimizing the free energy leads to a Maxwell construct for this system. Combining this cubic equation of state for the metastable region with the strong coupling and mean-field results away from the transition point provides an accurate, analytic description of the entire phase diagram in higher dimensions.

## 2. Analytic approximations

Lattice gauge theory is defined in terms of a partition function, from which all physical observables can be derived. The partition function is

$$\mathcal{Z}(\beta) = \int \mathcal{D}[\mathcal{U}] e^{-\beta \mathcal{S}[\mathcal{U}]}, \tag{1}$$

where  $\mathcal{U}$  is the set of all link variables  $U_l$ ,  $\mathcal{S}[\mathcal{U}]$  is the gauge invariant Wilson action and  $\mathcal{D}[\mathcal{U}] = \prod_l dU_l$  is the gauge invariant, normalized group measure. The link variable can be written as a complex phase,

$$U_l \equiv e^{i\phi_l}; \quad dU_l = \frac{d\phi_l}{2\pi}.$$

The integration is over  $\phi_l \in [0, 2\pi]$ . The parameter  $\beta$  is related to the bare coupling constant and the inter-site spacing,  $a$ , by

$$\beta = \frac{a^{d-4}}{e_0^2}.$$

In order to use the tools and insights of thermodynamics and statistical mechanics we associate  $\mathcal{Z}$  with the canonical partition function,  $\beta$  with an effective inverse temperature, and  $\mathcal{S}$  with the effective hamiltonian or energy. A free energy,  $\mathcal{F}$ , can also be defined from

$$\mathcal{Z}(\beta) \equiv e^{-\beta \mathcal{F}}.$$

The action is constructed to be gauge invariant and have the correct classical limit as  $a$  approaches zero<sup>1</sup>

$$\mathcal{S}[\mathcal{U}] = \sum_{\square} (1 - \text{Re } U_{\square}), \tag{2}$$

where

$$U_{\square} \equiv U_{ij} U_{jk} U_{kl} U_{li}$$

---

<sup>1</sup> This is the convention of Refs. [18, 19]. The constant can be removed from this action, which is often done, at the cost of changing some signs in the definition of the partition function. The plaquette energy is then reflected about the line  $E_{\square} = 0.5$ .

is the plaquette variable traversed once and the sum is over all plaquettes on the lattice. For this form of the action, the plaquette energy, defined as the average action per plaquette, has the limits  $E_{\square}(\beta \rightarrow 0) = 1$  and  $E_{\square}(\beta \rightarrow \infty) = 0$ .

Counting is important on the lattice since many of the interesting quantities scale with different properties of the lattice. The lattice used in this work is an isotropic,  $d$ -dimensional hypercube with  $n$  sites per side. This gives  $N_s = n^d$  sites,  $d$  links per site and  $d(d-1)/2$  plaquettes per site. The lattice spacing is the same in all directions corresponding to a zero physical temperature system.

The plaquette energy will be defined as

$$E_{\square} \equiv \langle \mathcal{S}_{\square} \rangle = \frac{2}{d(d-1)N_s} \frac{\partial (\beta \mathcal{F})}{\partial \beta}. \quad (3)$$

Both the strong coupling expansion and mean-field theory approximate the free energy. The plaquette energy, our order parameter, is then easily calculated using the above.

For a more detailed discussion of these methods see Refs. [14, 19, 20].

### 2.1. Strong coupling expansion

When the bare coupling,  $e_0$ , is large then the partition function, equation (1), can be expanded in a Taylor series in  $\beta \propto 1/e_0^2$  [3]. Series now exist to order  $\mathcal{O}(\beta^{16})$  for most groups and arbitrary dimension and to  $\mathcal{O}(\beta^{22})$  for  $U(1)$  in  $d = 4$  [3, 14]. (See Table I.)

TABLE I

Coefficients for the strong coupling expansion for the series  $\mathcal{F} = 1 - \sum_n c_n \beta^n$ . Taken from Ref. [14] (and independently verified by the author through  $n = 12$ ).

$n$	$c_n$	$n$	$c_n$
2	$\frac{1}{4}$	10	$\frac{d^2}{256} - \frac{85d}{6144} + \frac{2473}{204800}$
4	$\frac{1}{16}$	12	$-\frac{29d^2}{6144} + \frac{2467d}{131072} - \frac{1992533}{106168320}$
6	$\frac{d}{96} - \frac{11}{576}$	14	$\frac{5d^3}{2048} - \frac{237d^2}{16384} + \frac{178003d}{5898240} - \frac{38197099}{1734082560}$
8	$-\frac{d}{128} + \frac{757}{49152}$	16	$-\frac{15d^3}{4096} + \frac{1485d^2}{65535} - \frac{53956913d}{1132462080} + \frac{11483169709}{338228674560}$

This series has a finite radius of convergence. Even just a few terms is good enough to reproduce the Monte Carlo data for small  $\beta$ . However, as  $\beta$  approaches the phase transition the higher order terms dominate and destroy this agreement. Padé approximants can be used to improve the

behavior of the series near the critical value. In this work, the plaquette energy is calculated from the free energy series and the Padé approximant applied to the plaquette energy series. Only near diagonal approximants are used,  $P[m, m \pm 1]$ . The Padé approximant can be used for  $\beta < \beta_P$  where  $\beta_P$  is the smallest singularity in the Padé approximant on the real axis. These singularities are consistently above the numerically seen transition point.

## 2.2. Mean-Field Theory (MFT)

When  $\beta$  is large the only significant contribution to the partition function comes from when the action is near zero. This occurs for  $U_\square$  close to unity for all plaquettes, *i.e.*, all of the “plaquette angles” are aligned. Variational mean-field theory couples each link to an “external” field originating from the average interaction the link feels due to its coupling to neighbors. This is a good approximation if the plaquette variables are all close to the same value; therefore, MFT is valid as  $\beta \rightarrow \infty$ .

Mean-field theory is discussed and developed in Refs. [1, 2, 14, 19].

In addition to large  $\beta$ , a large number of neighbors should make MFT more appropriate. Staying with a hypercubical lattice, that means going to higher dimensions. We will utilize this by working in dimensions up to seven.

Many authors have previously looked at the effects of gauge fixing on MFT [7, 21, 22]. For completeness, the details of gauge fixing are discussed below. In the context of MFT, enforcing the axial gauge results in a lower bound on the free energy than no gauge fixing. There are some definite disadvantages to working in the axial gauge; however, none of them directly effect this work. The breaking of rotational symmetry on the lattice is aesthetically unsatisfying. In addition, higher order corrections within MFT are more difficult than in other gauge schemes. However, the simplicity of implementing the axial gauge at the tree level make it a compelling improvement for this work.

The axial gauge fixes all temporal links at unity resulting in the following self-consistent equations

$$H = 2(d-2)\beta u^3(H) + 2\beta u(H); \quad u(H) = \frac{I_1(H)}{I_0(H)},$$

where  $u(H)$  is the expectation value of a single link variable. The plaquette energy is then

$$E_\square = 1 - \frac{d-2}{d}u^4(H) - \frac{2}{d}u^2(H).$$

### 2.3. Gauge fixing

Before discussing gauge fixing, gauge transformations must be discussed. A gauge transformation is defined by assigning a phase,  $e^{ig_j}$ , to each site and then transforming the links via  $U_{jk} \rightarrow e^{ig_j} U_{jk} e^{-ig_k}$ . These gauge factors cancel in pairs along any closed curve. Hence, the plaquette variable, the action, and the energy per plaquette are all gauge invariant quantities. The individual link variables are *not* gauge invariant.

Gauge freedom allows some of the link variables to be fixed, leaving only integrals over the remaining links. Since the gauge group is compact, gauge transformations do not lead to divergences as in continuum QED and it is not necessary to fix the gauge. However, gauge fixing can be useful in some instances. The following argument is similar to Refs. [18, 23].

Let  $U_f$  be a link whose value is to be set to  $U_0$ . This is achieved with a gauge transformation. Consider a gauge invariant function

$$g = \int dU_f G(U_f),$$

where

$$G(U_f) = \int \prod_{l \neq f} dU_l g[\mathcal{U}] e^{-\beta \mathcal{S}[\mathcal{U}]}.$$

Note that  $G(U_f)$  is only a function of the link to be fixed. Applying the gauge transformation takes  $U_f \rightarrow U_0$ . Since  $g[\mathcal{U}]$  and  $\mathcal{S}[\mathcal{U}]$  are defined to be invariant,  $G(U_f) \equiv G(U_0) = \text{constant}$ . The gauge invariant function is now

$$g = G(U_0) \int dU_f = \int \prod_{l \neq f} dU_l g[\mathcal{U}'] e^{-\beta \mathcal{S}[\mathcal{U}]}$$

with  $\mathcal{U}'$  the gauge transformed links. The integration over  $U_f$  disappears since we are using a normalized measure. This can be repeated until all of the remaining unfixed links would close a loop on the lattice. These loops are gauge invariant and cannot be fixed. In the axial gauge used below,  $N_s$  links are fixed. The trial action for MFT becomes,

$$\beta \mathcal{S}_{\text{Axial}} \equiv \beta \sum_{\square(\text{sp})} (1 - \text{Re } U_{\square}) + \beta \sum_{\square(\text{t})} (1 - \text{Re } U_l U_{l'}) + H \sum_{l \in \text{sp}} \text{Re } U_l, \quad (4)$$

where the first term is the normal Wilson action for the spatial plaquettes, the second, the Wilson action for the temporal plaquettes with the time links set to unity and the final term, the external field coupling with just the spatial links. The MFT weight is adjusted analogous to the last term above.

What good is gauge fixing? In the Monte Carlo simulations, gauge fixing reduces the number of links to be tested per lattice sweep. However, this is not necessarily an improvement since the new configuration will not be as far away from the old configuration as if all of the links were tested. In Ref. [24] the authors argue that static gauge fixing slows down convergence for Monte Carlo calculations. In the strong coupling expansion, the isotropy of the lattice is useful so no fixing is used.

Mean-field theory is a different story. The above variational method can be implemented in a slightly different manner which evaluates the integrals using the method of steepest descent [7, 15]. In this case the gauge degrees of freedom correspond to zero-modes in the integrand leading to undesirable divergences when the limits in the steepest descent integrals are taken to infinity. Gauge fixing is required. In the above description, gauge fixing is not required. So the question becomes, if gauge fixing is not necessary, is it useful? Since the desired state is that which has the lowest free energy, the question becomes, does fixing the gauge lower the free energy? Working in the axial gauge, the bound on the free energy is lower than without gauge fixing.

Since any configuration on the unfixed lattice can be transformed into a configuration in the axial gauge, some of the link variables are not independent, dynamical degrees of freedom. In fact, all of the fixed links correspond to extraneous degrees of freedom. Therefore, the manifestly gauge invariant Wilson action includes  $N_s$  non-dynamical degrees of freedom. By removing the extraneous degrees of freedom, the trial action is closer to the true answer and hence gives a better variational bound on the free energy.

Other choices of gauge fixing exist [7, 25, 26]. The Feynman gauge [7] is appealing for its covariant nature, but is not a simple to implement. Two methods, Landau [25] and Laplacian [26] gauges, are dynamical gauge fixings and not easily implemented in MFT.

### 3. Numeric results

In order to test the analytic methods, exact, numeric data are needed. New Monte Carlo calculations of the plaquette energy are performed in six and seven dimensions. The code is an extension of work by Dubach [27].

A simple Metropolis algorithm is used with one hit per test and weighting of the new link value to lie close to the old value. A typical run consisted of 1000–50000 sweeps over the lattice depending on how quick convergence was. Block averaging was used to account for correlations between sweeps. *Error bars are smaller than plotted points on all figures shown.* Both heating, decreasing  $\beta$ , and cooling, increasing  $\beta$ , runs were made near the transition point to check for hysteresis loops. Various lattice sizes were used to check

for significant finite-size effects. Small effects were seen in four dimensions with negligible effects in higher dimensions. Calculations were carried out for the following lattice sizes:  $5^4, 8^4, 10^4, 5^5, 8^5, 5^6$  and  $5^7$ .

To test the numeric calculation the phase diagram for four dimension was reproduced and compares well with that of Lautrup and Nauenberg [10]. The data below  $\beta = 0.5$  were also compared to the SCE where agreement is expected to be very good.

The phase diagram for five dimensions showed regions of metastability and compares favorably with that of Bhanot and Creutz [9]. The phase diagram for six dimensions is similar to that for five dimensions, showing a hysteresis loop. This is indicative of a first order phase transition. The jump in plaquette energy is larger than in five dimensions suggesting that the transition is becoming stronger. The phase diagrams for four and six dimensions are shown in figure 1.

The critical value is also moving towards zero. As the dimension goes to infinity, both SCE and MFT predict a critical value of  $\beta = 0$  and a discontinuity of  $\Delta E_{\square} = 1$ .

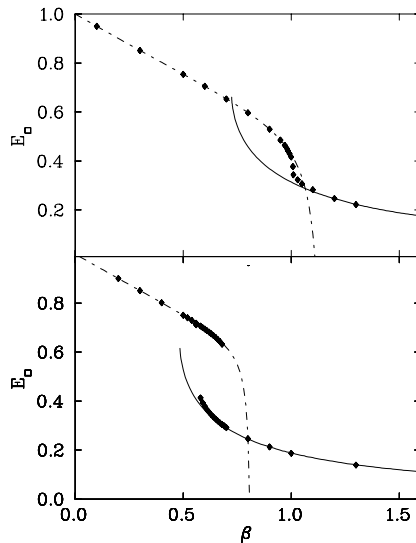


Fig. 1. Phase diagram for 4- $d$  (upper frame) and 6- $d$  (lower frame) U(1) LGT. The diamonds are Monte Carlo data on  $8^4$  and  $5^6$  lattices respectively. The solid line is MFT in the axial gauge and the dash-dot line is the [7,8] Padé approximant. Notice the appearance of a metastable region near  $\beta = 0.75$  in the 6- $d$  case.

#### 4. Bridge

In Section 2, two analytic methods were presented to approximate the phase diagram for a U(1) lattice gauge theory. The strong coupling expansion with Padé approximants works well below the transition point and even reproduces the supercooled region in the higher dimensions. Mean-field theory with axial gauge fixing reproduces the weak coupling region including the superheated phase. Now we wish to build a bridge between these two descriptions.

It is known that the four dimensional U(1) theory exhibits either a second order or weak first order transition. This transition region has been well studied previously [10,28,29] and the critical value is  $\beta_c \approx 1.011$  [29]. However, it is unreasonable to expect the analytic methods to predict a second order transition. Long-range correlations come into play and neither method can handle them accurately. In larger dimensions the transition is first order; there are no long-range correlations and the analytic methods are accurate well into the metastable regions. Therefore, the bridging method will be developed in higher dimensions. In the end, this technique will be applied in four dimensions to see how well it works.

Where metastable states exist it is clear that the plaquette energy is not a true function of  $\beta$ ; rather, it is multivalued. However, one might suspect that  $E_\square$  is a continuous, single-valued function of  $\beta$ . This would be analogous to the Van der Waal's equation of state where the pressure is a unique function of the volume but there are regions where the volume is a multivalued function of the pressure. There is then a physically unstable region where  $E_\square$  increases with  $\beta$ ; the specific heat is negative. Since this region cannot be explored using the numeric techniques discussed above, a simple parameterization will be used to describe the unphysical region<sup>2</sup>. The cubic is the lowest order polynomial with the desired shape to fit the metastable states and the unphysical state. Therefore, the data in the multivalued region will be fit with a cubic  $E_\square(\beta) = \mathcal{O}(\beta^3)$ . The relative free energy comes from integrating  $E_\square$  along this curve,

$$\Delta \left( \frac{\beta \mathcal{F}}{N_s} \right) = \int_a E_\square d\beta.$$

Integrating  $E_\square$  along this curve gives the exact free energy relative to the lower bound of the integral. A crossing in the free energy curve is seen as shown in figure 2 (see also Ref. [32]). The free energy is also a multivalued

---

<sup>2</sup> Methods for exploring this region numerically with a microcanonical ensemble have been suggested by Hetherington and Stump [30] for the U(1) model and by Challa and Hetherington [31] for the related Potts models.

function of  $\beta$ . The preferred phase is the one with lowest free energy. This defines a Maxwell construction. This crossing point identifies the point of phase transition.

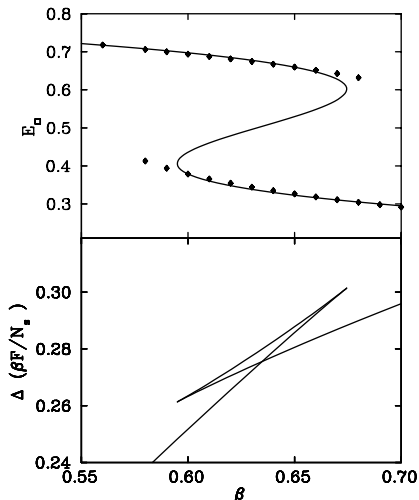


Fig. 2. The upper frame shows the cubic fit in the metastable region for the 6-d phase diagram. The lower frame shows the relative free energy obtained by integrating the plaquette energy along the upper curve. The system favors the phase with lowest free energy and thus changes phase where the lower two lines cross.

This method gives a clean signal of the transition that is in line with previous techniques. The critical values predicted with this method and some previous results are compared in Table II. The  $\beta_c^{\text{cubic}}$  values are from this work using the cubic equation of state and Maxwell construction as described above. The four dimensional Monte Carlo “other” results are from Ref. [29]; the five dimensional result is from Ref. [9]. In six dimensions the method of Bhanot and Creutz [9] gives  $\beta_c = 0.64$ . The  $\beta_c^{\text{F1}}$  values are taken from Ref. [7] where corrections to MFT were calculated to fourth-order in one over the mean-field strength and then a direct matching of the predicted free energies was used to find the transition point.

This method can also be used in four dimensions. To the accuracy of the Monte Carlo calculations in this study, the transition appears to be second order. A second order transition will show a inflection point at the critical value and no crossing of the free energy. In other words,  $\partial\beta/\partial(E_\square)$  should be zero. Since a finite size lattice cannot show a true phase transition, we find for a  $8^4$  lattice a slope of  $-0.00654$  at a critical value  $\beta_c(8^4) = 1.004$ . This critical value is in reasonable agreement with that of Klaus and Roiesnel [29] who find  $\beta_c(8^4) = 1.007$ .

TABLE II

Comparison of critical coupling values

Lattice size	Monte Carlo		Analytic	
	$\beta_c^{\text{cubic}}$	$\beta_c^{\text{others}}$	$\beta_c^{\text{cubic}}$	$\beta_c^{\text{Fl}}$
$5^4$	0.995(1)	0.9985(4) [29]	0.88(1)	1.00 [7]
$8^4$	1.004(1)	1.007(1) [29]	0.88(1)	1.00 [7]
$5^5$	0.751(2)	0.736(5) [9]	0.742(5)	0.758 [7]
$5^6$	0.634(5)	—	0.652(5)	—

Riding on the successes in matching the phases and finding critical values for the Monte Carlo data, the same technique is applied to the analytic methods. However, a difficulty immediately arises, where do the analytic curves end? For the Monte Carlo data there is a definite point where the superheated phase ends. It occurs when there is a sudden change in the plaquette energy and the energy is the same as in the hot phase. Such a signal does not exist for the analytic curves. Since it is desirable to have an analytic method which is independent of the Monte Carlo data, we cannot use the actual ends of the metastable regions. Also, since one of the goals is to find the critical coupling, the method needs to be independent of  $\beta$ . One such unambiguous method is to require that the slopes of the curves match at the cutoff points. This is a simple, *ad hoc* method that satisfies the requirements and the results can be checked against the Monte Carlo results. The cutoff slope is chosen so there is some overlap between the two phases. The two curves are then fit with the cubic in the range between the two cutoff couplings. Variations in the value of the cutoff slope make only small changes in the calculated critical value. The analytic phase diagram then consists of the Padé approximants to the strong coupling expansion for  $\beta \leq \beta_c$ , a phase transition at  $\beta_c$  and mean field theory in the axial gauge for  $\beta \geq \beta_c$ . An example for six dimensions is shown in figure 3.

Attempts to apply this method to the analytic approximations in four dimensions do not meet with the success seen in higher dimensions. The predicted critical value is too low by at least 10% in four dimensions. A careful study of the four dimensional phase diagram reveals why. Near the critical point for a second order transition long-range correlations are important. The SCE accounts for some of this with terms corresponding to extended shapes. For example, there is a diagram that contributes at 14<sup>th</sup> order which is a cylinder connecting plaquettes three sites apart. Larger order series include longer range connections. In contrast, MFT reduces the problem to a local one-body problem; effects arising from scales larger than

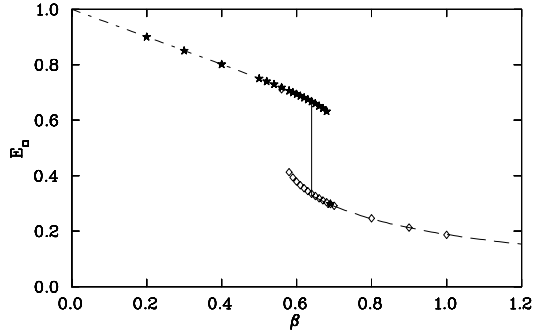


Fig. 3. Analytic phase diagram in six dimensions. Dash-dot line is Padé series for SCE up to the transition point, the solid vertical line marks the transition point and the long-dashed line is axial MFT beyond the transition point. Also shown are the Monte Carlo data.

nearest neighbor are lost in MFT. Mean-field theory is better near a strong first-order transition than a second-order transition. When the plaquette energy increases near the critical point due to correlation effects, MFT can not keep up and the analytic prediction is moved to lower  $\beta$ .

## 5. Conclusions

The goal of this work has been to develop an analytic description of the U(1) phase diagram in arbitrary dimension. Many methods have been developed over the years to tackle this problem. Two of the earliest methods, strong coupling expansion and mean-field theory, are found to need only minor adjustments to be in excellent agreement with Monte Carlo calculations. A consistent, physically motivated procedure is developed to connect one description to the other in the region of the phase transition. To do this, similarities between the U(1) phase diagram and that of the Van der Waal's equation of state are exploited.

In large dimensions, numeric simulations of U(1) LGT show a first order transition with long-lived metastable phases. This is exactly what occurs near the transition region for a Van der Waal's system. It is postulated that in the metastable region there exists an additional state which is physically unstable and numerically unreachable with the canonical partition function used here. It is noted again in passing that microcanonical methods have been developed which show this unstable state [30]. As in the Van der Waal's equation of state, the U(1) system is modeled as being cubic in the inverse coupling squared. The coefficients in this cubic equation of state are fit to the data for the metastable states in the region of the transition. The

relative free energy is found by integrating along the equation of state and shows a point where the phase with lowest free energy changes. This defines the transition point. This technique allows for the accurate identification of the transition point of a first-order phase transition.

The success of the analogy to the Van der Waal’s system suggests using this technique to connect the two analytic descriptions. The strong coupling expansion to at least order  $\mathcal{O}(\beta^{16})$  is used. Padé approximants are constructed to take into account singularities in the series. *The results are in excellent agreement with numeric data from small  $\beta$  past the transition point into the supercooled phase.* Variational mean-field theory is applied to the large  $\beta$  region. It is found that gauge fixing improves the bounds on the free energy by removing non-independent degrees of freedom from the problem. The axial gauge is used giving the lowest upper bound on the free energy. *Mean-field theory is then in agreement with the Monte Carlo data from large  $\beta$  down past the transition region through the superheated phase.* Its only failure is in accounting for the long range correlations that develop near the second-order (or weak first-order) transition in four dimensions. The application of the above method of fitting a cubic equation of state gives transition points in excellent agreement with those from the Monte Carlo data.

As a final test of these methods, strong coupling and MFT calculations were done for seven dimensions and the transition point found at  $\beta = 0.583(2)$ . Monte Carlo runs were then performed on a  $5^7$  lattice for couplings near the transition point. The results are shown in figure 4. The analytic predictions are in *excellent agreement* with the Monte Carlo calculations well beyond the transition point. Agreement between predictions for the critical value is as good as in five and six dimensions.

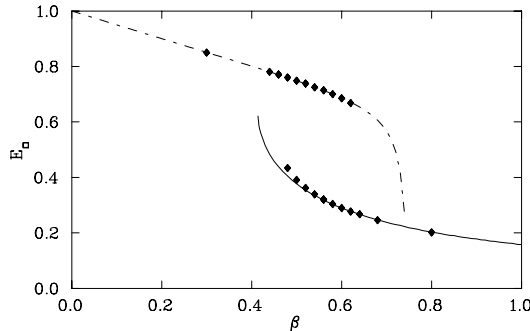


Fig. 4. Phase diagram for seven dimensional U(1) LGT. Diamonds are Monte Carlo data on a  $5^7$  lattice. Solid line is axial MFT and dash-dot line is the [7,8] Padé approximant for the SCE.

In this paper a method to describe the entire  $U(1)$  lattice gauge theory phase diagram analytically has been developed. The method is particularly successful in higher dimensions where there is a strong first-order phase transition. The use of strong coupling expansions and variational mean-field theory should allow these techniques to be extended to other Abelian and non-Abelian groups where these analytic methods have also been developed. A completely analytic description could be used as a launching pad for more in-depth analytic and numeric studies of lattice gauge theories.

The author would like to thank John Dubach for the original Monte Carlo code used in this work, Dirk Walecka for his guidance and insight and Shiwei Zhang for many fruitful discussions. This work was supported by a fellowship from the Southeastern Research Universities and Thomas Jefferson National Accelerator Facility.

## REFERENCES

- [1] K. Wilson, *Phys. Rev.* **D10**, 2445 (1974).
- [2] R. Balian, J.-M. Drouffe, C. Itzykson, *Phys. Rev.* **D10**, 3376 (1974).
- [3] R. Balian, J.-M. Drouffe, C. Itzykson, *Phys. Rev.* **D11**, 2104 (1975).
- [4] M. Falcioni, E. Marinari, M.L. Paciello, G. Parisi, B. Taglienti, *Phys. Lett.* **B105**, 51 (1981).
- [5] R. Hornsley U. Wolff, *Phys. Lett.* **B105**, 290 (1981).
- [6] N.D. Hari Dass, P.G. Lauwers, A. Patkós, *Phys. Lett.* **B124**, 387 (1983).
- [7] H. Flyvberg, *Nucl. Phys.* **B235 [FS11]**, 331 (1984).
- [8] A. Duncan, H.F. Jones, *Nucl. Phys.* **B320**, 189 (1989).
- [9] G. Bhanot, M. Creutz, *Phys. Rev.* **D21**, 2892 (1980).
- [10] B. Lautrup, M. Nauenberg, *Phys. Lett.* **B95**, 63 (1980).
- [11] B. Berg, C. Panagiotakopoulos, *Phys. Rev. Lett.* **52**, 94 (1984).
- [12] L. Del Debbio, A. Di Giacomo, G. Paffuti, *Phys. Lett.* **B349**, 513 (1995).
- [13] J. Cox, W. Franzki, J. Jersák, C.B. Lang, T. Neuhaus, P.W. Stephenson, *Nucl. Phys.* **B449**, 371 (1997).
- [14] J.-M. Drouffe, J. Zuber, *Phys. Rep.* **102**, 1 (1983).
- [15] C. Itzykson, J.-M. Drouffe, *Statistical Field Theory*, Cambridge University Press, Cambridge 1989, Vol. 1.
- [16] B. Lautrup, W. Rühl, *Z. Phys.* **C23**, 49 (1984).
- [17] P.Y. Zhou, J.M. Wu, *Nucl. Phys. B Proc. Suppl.* **53**, 719 (1997).
- [18] I. Montvay, G. Münster, *Quantum Fields on a Lattice*, Cambridge University Press, Cambridge 1994.

- [19] J.D. Walecka, *Theoretical Nuclear and Subnuclear Physics*, Oxford Univ. Press, Oxford 1995.
- [20] J.B. Kogut, *Rev. Mod. Phys.* **55**, 775 (1983).
- [21] J. Greensite, B. Lautrup, *Phys. Lett.* **B104**, 41 (1984).
- [22] D. Brout, R. Brout, M. Puolain, *Nucl. Phys.* **B205**, 233 (1982).
- [23] M. Cruetz, *Quarks, Gluons and Lattices*, Cambridge University Press, Cambridge 1983.
- [24] B. Lautrup, M. Lavelle, M. Tuite, A. Vladikas, *Nucl. Phys.* **B290**, 188 (1987).
- [25] M.I. Polikarpov, K. Yee, M.A. Zubkov, *Phys. Rev.* **D48**, 3377 (1993).
- [26] J. Vink, *Phys. Rev.* **D51**, 721 (1995).
- [27] J. Dubach, private communication.
- [28] M. Baig, *Nucl. Phys. B Proc. Suppl.* **42**, 654 (1995).
- [29] B. Klaus, C. Roiesnel, High-statistics finite size scaling analysis of U(1) lattice gauge theory with Wilson action, hep-lat/9801036, 1998.
- [30] J.H. Hetherington, D.R. Stump, *Phys. Rev.* **D35**, 1972 (1987).
- [31] M.S.S. Challa, J.H. Hetherington, *Phys. Rev.* **A38**, 6324 (1988).
- [32] F. Reif, *Fundamentals of Statistical and Thermal Physics*, McGraw-Hill, Inc., New York 1965.